



# Removal of metal ions from aqueous solutions using carboxymethyl cellulose/sodium styrene sulfonate gels prepared by radiation grafting



Tran Thu Hong<sup>a,b,\*</sup>, Hirotaka Okabe<sup>a</sup>, Yoshiki Hidaka<sup>a</sup>, Kazuhiro Hara<sup>a</sup>

<sup>a</sup> Department of Applied Quantum Physics and Nuclear Engineering, Faculty of Engineering, Kyushu University, 744 Motoooka, Fukuoka 819-0395, Japan

<sup>b</sup> Nuclear Research Institute, Vietnam Atomic Energy Institute (VINATOM), 01 Nguyen Tu Luc, Dalat, Lam Dong, Vietnam

## ARTICLE INFO

### Article history:

Received 2 June 2016

Received in revised form

11 September 2016

Accepted 15 September 2016

Available online 16 September 2016

### Keywords:

$\gamma$ -Radiation

Carboxymethyl cellulose

Sodium styrene sulfonate

Hydrogel

Grafting

Metal adsorption

## ABSTRACT

Sodium Carboxymethyl Cellulose (CMC–Na)/Sodium Styrene Sulfonate (SSS) hydrogels with grafted and crosslinked polymeric networks were prepared by  $\gamma$ -radiation at atmosphere condition. The obtained hydrogels were characterized by gel fraction, swelling ratio, TGA and FTIR spectroscopy. The results showed the ratio of CMC and SSS 1:0 gave the highest gel fraction, compared with other ratios. The swelling capacity increased by increasing SSS content due to the presence of  $-\text{SO}_3\text{Na}$ ,  $-\text{OH}$  groups in gel structure. The FTIR spectrum of CMC/SSS gel showed the new absorption peaks at 1034 and 1012  $\text{cm}^{-1}$  corresponds to  $-\text{SO}_3\text{Na}$  group. The metal ion adsorption capacity of CMC/SSS gel was investigated. The grafted gel effectively removed metal ions, especially Cr and Pb. The effects of hydrogel composition, contact time, and initial concentration on the adsorption capacity of the grafted hydrogels were studied. The adsorption kinetics and equilibrium isotherms were investigated using pseudo-second-order model and Langmuir model.

© 2016 Published by Elsevier Ltd.

## 1. Introduction

Water sources like lakes, sea, groundwater, etc. are becoming polluted by different kinds of contaminants, including toxic heavy metals (e.g., Cr, Pb, Cu, Ni, Cd, Fe, etc.) accidentally and deliberately discharged into these surface waters by commercial and industrial establishments. The resulting environmental hazards are undesirable and therefore heavy metal ions must be appropriately removed using new/improved techniques. Currently, many methods are being used to remove heavy metal ions from wastewaters such as chemical precipitation, reverse osmosis, membrane filtration, and electro-chemical treatment technologies (Barakat, 2011). However, the effectiveness of these methods is limited in the case of low metal ion concentration. Adsorption method using polymeric material is one of the important alternatives available for such situation (Crini, 2005). A variety of low cost adsorbent materials from natural polymers has been considered because of their excellent properties of complexation, flocculation, chelation, separation, and adsorption of a whole range of pollutants.

Cellulose and its derivatives have received much attention recently because they are naturally found. As such they are biodegradable and relatively safe (Sultana, Islam, Dafader, & Haque, 2012) in addition to their unique structure and distinctive properties. Carboxymethyl cellulose (CMC) especially, is a strong adsorbent for removal of a wide range of heavy metal ion pollutants such as U (II) (Ma, Hsiao, & Chu, 2012), Ag (I), Fe (III), Cu (II) (Liu et al., 2015), Ni (II), Cr (III) and Zn (II) (Sehaqui et al., 2014). Wang et al. (Wang & Wang, 2011) observed that the presence of reactive carboxymethyl groups ( $-\text{CH}_2\text{COOH}$ ) render the CMC soluble, chemically reactive and strongly chelating and this makes the application of CMC in adsorbent fields more attractive and promising. Furthermore, the useful properties of cellulose and CMC can be improved via graft polymerization with hydrophilic vinyl monomers such as acrylic acid (AA) (Gu, 2001), acryl amide (AAM) (Ghosh, Dev, & Samanta, 1995), acrylonitrile (Gupta & Sahoo, 2001) and acrylate (Mondal, 2013). CMC-g-Poly (AA) gels have showed higher flocculation efficiency than CMC itself reflecting the role of poly (AA) in river water clarification (Mishra, Rani, & Sen, 2012). Hydrogels prepared from CMC and AAM are efficient adsorbents with 80.31% reduction in turbidity of kaolin suspension whereas the turbidity capacity of CMC hydrogels is 13.75% (Ogbeifun & Okieimen, 2004).

Another vinyl monomer also containing hydrophilic group but has not been much considered is sodium styrene sulfonate (SSS). The main advantages of SSS as compared to other monomers are

\* Corresponding author at: Department of Applied Quantum Physics and Nuclear Engineering, Faculty of Engineering, Kyushu University, 744 Motoooka, Fukuoka 819-0395, Japan.

E-mail address: [hong@athena.ap.kyushu-u.ac.jp](mailto:hong@athena.ap.kyushu-u.ac.jp) (T.H. Tran).

**Table 1**  
Initial concentration of metal ions for adsorption (ppb).

Metal	Pb(II)	Cu(II)	Zn(II)	Cd(II)	U(V)	Cr(III)	Mo(II)	Mn(II)	Fe(II)	Ni(II)
Conc. (ppb)	10	100	100	3	2	50	70	50	300	10

higher reactivity, low toxicity and high thermal stability (Korus, 2012). SSS is also classified as a good vinyl monomer for preparing polyelectrolyte complex hydrogels by mixing with polysaccharides (Kumar, Setia, & Mahadevan, 2012). On the basis of above background, a series of gamma radiation induced CMC/SSS hydrogels were prepared and used as adsorbents for heavy metal ions adsorption from aqueous solution. The parameters influencing the adsorption capacity of grafted gels such as SSS content, contact time, and initial concentration were investigated.

## 2. Experimental

### 2.1. Materials and reagents

Sodium carboxymethyl cellulose (CMC–Na;  $M_w \sim 700,000$ ) was obtained from Alfa Aesar (England). Sodium 4-Styrenesulfonate monomer (SSS) and the multi-element metal ion stock solution TraceCERT® were purchased from Fluka, Sigma-Aldrich (Switzerland). Water was used in all experiments purified by Puric ω (Organo, Japan). All other reagents such as Sodium hydroxide and Hydrochloric acid were analytical grade and used as received without further purification.

### 2.2. Preparation of the copolymer hydrogels

A series of hydrogels were prepared by the following procedure. An aqueous solution of 20 wt% CMC/SSS in paste-like state with different compositions was put into polypropylene tubes. Each mixture was centrifuged at 10,000 rpm for at least 5 h using HSIANGTAI Model CN-1050 (Taiwan) in order to remove tiny bubbles. After the  $\gamma$ -ray irradiation from 20 to 100 kGy by the  $^{60}\text{Co}$  source of Kyushu University's Center for Accelerator and Beam Applied Science, the irradiated gels were extracted, washed with distilled water to remove un-reacted component. The particles size fraction 5 mm<sup>3</sup> ( $\sim 0.20$  g) was chosen for all experiments.

### 2.3. Characterization

#### 2.3.1. Gel fraction and swelling properties

The gel content in the sample was estimated by measuring its insoluble part gravimetrically after the extraction in distilled water at room temperature for 48 h. The gelled parts were dried to constant weight at 50 °C. Gel fraction was determined from the following Eq. (1):

$$\text{Gel fraction(\%)} = \frac{W_d}{W_0} \times 100 \quad (1)$$

where  $W_d$  (g) is the weight of dried gel after extraction and  $W_0$  (g) the initial weight of dry gel.

The grafted hydrogels were soaked in distilled–deionized water for a certain time at room temperature. After wiping excess water at the surface of the gel, the weight of swollen gel was measured. Swelling ratio ( $S_w$ ) of the blend hydrogels was calculated from the following Eq. (2):

$$S_w (\text{g/g}) = \frac{W_s - W_d}{W_d} \quad (2)$$

where  $W_s$  (g) is the weight of the swollen gel and  $W_d$  (g) the weight of dried gel.

#### 2.3.2. Fourier transforms infrared (FTIR) and carbon-13 nuclear magnetic resonance ( $^{13}\text{C}$ NMR) spectroscopy analysis

FTIR analysis was performed to determine the nature of modification of CMC/SSS hydrogels by using the FTIR (Jasco FT/IR 4100, Japan) ATR method in the range from 400 to 4000  $\text{cm}^{-1}$ .

$^{13}\text{C}$  NMR spectrum was recorded on a JEOL JNM-ECA-400 NMR spectrometer. (Japan).

#### 2.3.3. Thermo-gravimetric analysis (TGA) and scanning electron microscopy (SEM)

The CMC and CMC/SSS hydrogels were dried in vacuum oven at 50 °C for several days. TGA of hydrogels was performed on Jupiter STA 449 F3 over a temperature range of 20–800 °C with heating rate of 5 °C/min and nitrogen flow rate of 40 mL/min.

The surface morphology SEM of CMC and CMC/SSS hydrogels were taken with a Shimadzu SS-550S instrument (Japan). The coater was used to pre-coat conductive carbon onto surface before observing the microstructure at 15 kV.

### 2.4. Adsorption procedure

Batch adsorption experiments were carried out with a known mass of adsorbent was dipped into concentrated analyte solutions in closed vessels at room temperature of 25 °C. The grafted gel (0.20 g) was initially pre-treated in  $10^{-4}$  M sodium hydroxide solution for at 24 h prior to immersion into 30 mL of multi-element solution containing different initial concentration of metal ions shown in Table 1 for 24 h. The remaining metal ions in aqueous solution were determined by inductively coupled plasma mass spectrometer (ICP-MS, Agilent 7700X, Japan). The amount of heavy metals adsorbed at equilibrium and the percentage of metal ion removal in multi-element adsorption studies were interpreted as follows (3):

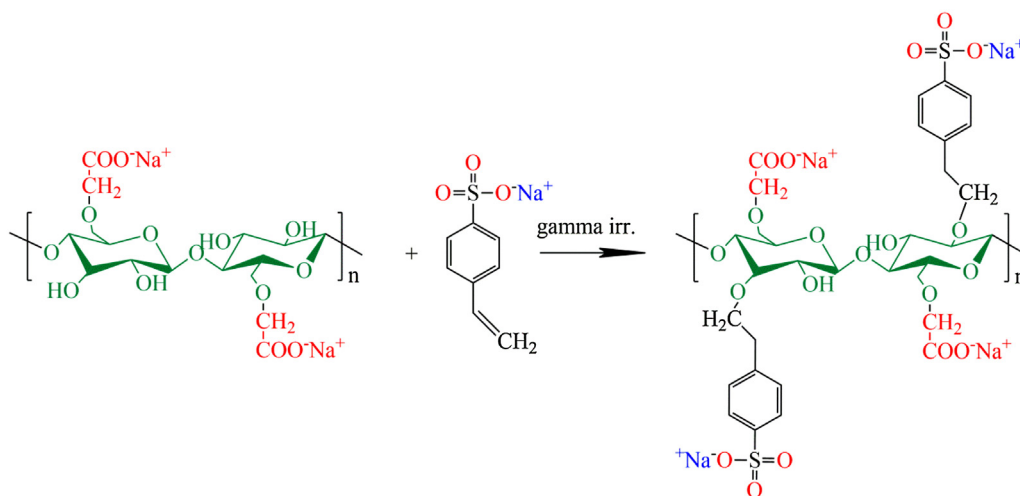
$$q_e = \frac{V(C_0 - C_e)}{w} \text{ and } \% \text{ removal} = \frac{C_0 - C_f}{C_f} \quad (3)$$

where,  $q_e$  is the amount of adsorbed metal ion at equilibrium (metal adsorption capacity) in  $\mu\text{g/g}$ ;  $V$  is the volume of adsorption medium in liter;  $C_0$ ,  $C_e$ ,  $C_f$  are the initial, equilibrium and final metal ion concentration in  $\mu\text{g/L}$ , respectively and  $w$  the weight of dried gel in grams. All tests were carried out at least three times and average was used in the analysis.

## 3. Results and discussion

### 3.1. Synthesis of CMC/SSS graft copolymer

The mechanism of synthetic vinyl monomer grafting onto polysaccharides using  $\gamma$ -radiation as the initiator has been well studied (Abd El-Mohdy, 2007). Scheme 1 shows the brief proposed synthesis of the graft copolymers based on CMC and SSS by using  $\gamma$ -radiation. At first, under  $\gamma$ -radiation, water molecules generate many energetic species including  $\text{HO}^\bullet$  and  $\text{H}^\bullet$  radicals. Then, those  $\text{HO}^\bullet$  and  $\text{H}^\bullet$  radicals extract H atoms from hydroxyl group of CMC chains and vinyl group of SSS to form the new CMC radicals and SSS radicals (Bao, Ma, & Li, 2011; Rivas & Muñoz, 2009). And thereafter, random reactions of these radicals leads to CMC/SSS graft copolymer which allows the production of much perfect network of higher cross-linking and grafting density.



**Scheme 1.** A brief proposed mechanism for irradiation-induced grafting of SSS onto CMC.

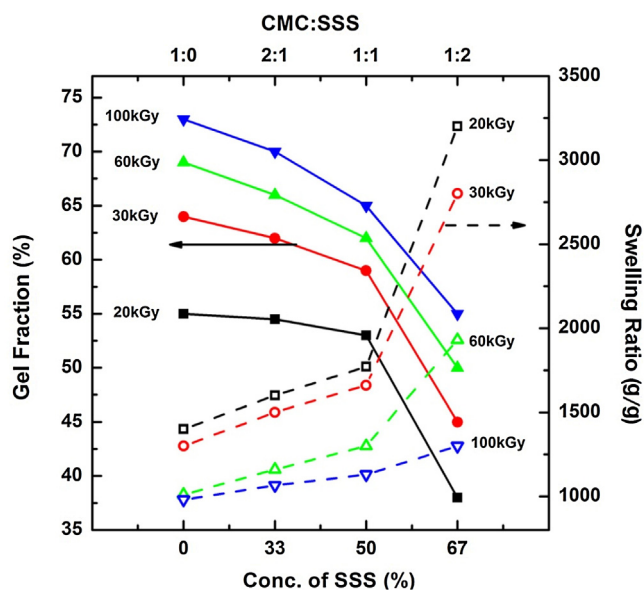


**Fig. 1.** Gel fraction and swelling ratio versus SSS concentration.

## 3.2. Characteristics of grafted gels

### 3.2.1. Effect ratio of CMC and SSS on gel fraction and swelling ratio

The effect of SSS has been investigated on the gel fraction by varying the concentration of SSS as shown in Fig. 1. It was observed that by increasing the concentration of SSS, the content of gel decreases constantly. The observed decrease in gel fraction is mainly due to the presence of CMC. In aqueous paste-like condition CMC radicals overlap and coil up and then, entangle to become a gel. Similar results have been reported on aqueous state radiation of CMC (Yoshii et al., 2003). It also was found that as high the concentration of monomer SSS leads to graft onto the CMC backbone readily.

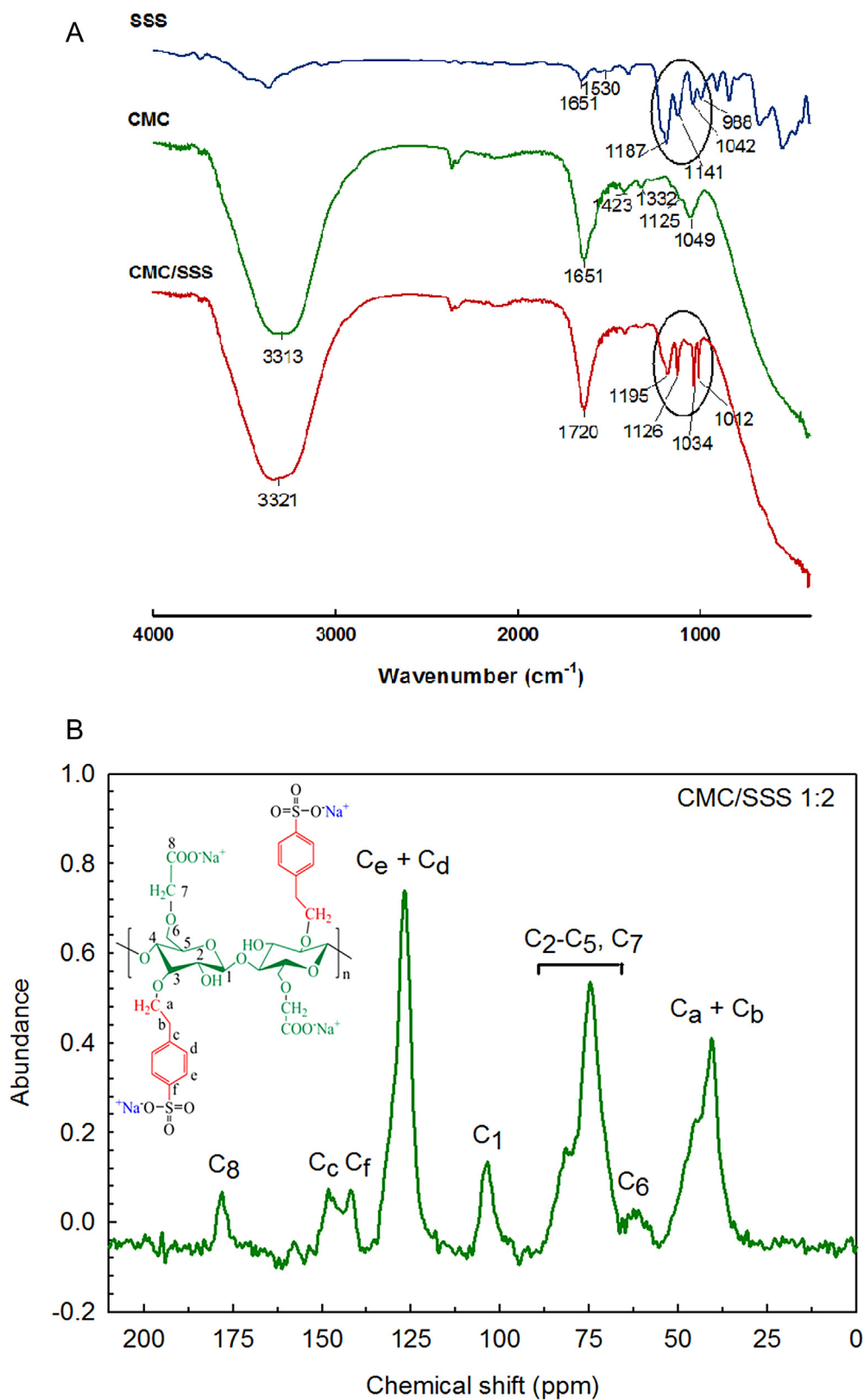
Swelling ability  $S_w$  is one of the most important properties of polymer adsorbents because it allows the diffusion of metal ions into the pores of gels and then favors the interaction of ions with active sites. Fig. 1 also shows the results of water adsorption capacity versus SSS concentration. In contrast with the decrease in the gel fraction, the  $S_w$  increased with increasing the SSS content. The highest swelling capacity was found for CMC/SSS gels with ratio of 1:2

while the lowest value corresponds to gels with ratio of 1:0. Since SSS is a hydrophilic monomer, it increases the water adsorbing capacity and water retention character of grafted gels. The presence of SSS is responsible for maximum hydrophilic character in grafted gels thereby increasing the ability of absorbing and retaining water. In other words, as the weight ratio of SSS to CMC increases, more SSS molecules could be available in the vicinity of the chain propagating sites of CMC macro radicals as well as increase hydrophilic groups such as  $-\text{SO}_3\text{Na}$ ,  $-\text{OH}$  which enhances the hydrophilicity of the corresponding superabsorbent hydrogels, and then the swelling capacity is improved. A similar result has been reported by B. Rivas et al. (Morales & Rivas, 2014). The degree of swelling decreases at the expense of increasing polymer volume fraction in the gel and network chain density. These results are reasonable.

### 3.2.2. FTIR and C NMR spectra

Infrared spectra of CMC, SSS and CMC/SSS are illustrated in Fig. 2(A). The FTIR spectrum of CMC shows the strong peak around  $3313\text{ cm}^{-1}$  due to the free O–H stretching vibration as well as inter- and intra-molecular hydrogen bonds in cellulose molecules (Pushpamalar, Langford, Ahmad, & Lim, 2006). The band at  $1651\text{ cm}^{-1}$  confirmed the presence of  $\text{COO}^-$  and assigned to stretching of the carboxyl group. The band at  $1423\text{ cm}^{-1}$  and  $1332\text{ cm}^{-1}$  was assigned to O–H stretching in-plane and C–H stretching in symmetric of CMC. The main characteristic band of SSS at  $1042$  and  $988\text{ cm}^{-1}$  ( $-\text{SO}_3\text{Na}$  group),  $1187$  and  $1141\text{ cm}^{-1}$  ( $\text{S}=\text{O}$  stretch) and  $1651$ ,  $1530$  &  $1400\text{ cm}^{-1}$  ( $-\text{C}_{\text{ar}}-\text{C}_{\text{ar}}$  bonds) are also shown. In the spectrum of grafted gels, in addition to the characteristic bands of CMC, new absorption peaks were observed. The new band at  $1034$  and  $1012\text{ cm}^{-1}$  corresponds to  $-\text{SO}_3\text{Na}$  group while the bands detected at  $1195$  and  $1126\text{ cm}^{-1}$  are due to  $\text{S}=\text{O}$  stretching vibration to confirm the presence of function groups responsible for the adsorption of metal ions.

The  $^{13}\text{C}$  NMR for CMC/SSS (Fig. 2(B)) shows peaks at  $103.6$  ( $\text{C}_1$ );  $81.6$  and  $74.7$  ( $\text{C}_2-\text{C}_5$ ) and  $361.41$  ( $\text{C}_6$ ) ppm respectively attributed glucosamine ring of cellulose. The signal at  $178.1$  ppm corresponds to the carbonyl carbon ( $\text{C}_8$ ) in the anionic  $-\text{COO}^- \text{Na}^+$  groups. Peaks at  $45.0$  and  $40.6$  ( $\text{C}_a$ ,  $\text{C}_b$ ) ppm are attributed to the carbon of SSS which are closest to the ether linkage with CMC. Peaks at  $148.2$  ( $\text{C}_c$ ) and  $126.8$  ( $\text{C}_d$ ,  $\text{C}_e$ ) ppm are attributed to the aromatic carbons of the SSS unit. The signal at  $141.9$  ppm is in good agreement with the chemical shift expected for a  $\text{C}_f$  for a sulfonic acid group. These spectral results confirmed the presence of both CMC and SSS in the CMC/SSS hydrogel, i.e. SSS was grafted successfully onto CMC backbone.



### 3.2.3. Thermo-gravimetric analysis (TGA) and scanning electron microscopy (SEM)

The formation of grafted gels between CMC and SSS was checked by thermo-gravimetric analysis in comparison with only CMC. The TGA curves of CMC and CMC/SSS gels are shown in Fig. 3. Two stages

of mass loss were observed in the TGA curves of CMC and CMC/SSS gel. The weight loss of CMC gel consists of the following stages: first 15% for the evaporation and the de-crosslinking in the temperature range 17–220 °C and another 30% for the thermal decomposition in the range 220–290 °C. Similarly, CMC/SSS first lost 30% weight

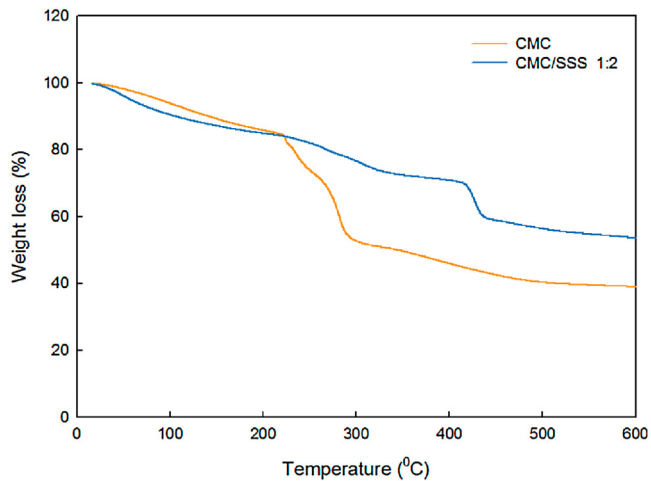


Fig. 3. TGA profile.

from 17 to 415 °C and then lost 10% weight from 415 to 440 °C. The results indicate that CMC/SSS gel has much bounding water by its stronger hydrophilicity although both were dried for 24 h at 50 °C in the vacuum oven. Fig. 3 also shows the temperature decomposition of SSS in grafted polymer is higher than temperature decomposition of pure CMC.

Examination of CMC and CMC/SSS hydrogels using SEM microscopy revealed more information regarding their surface morphology. As it can be seen in the SEM image (Fig. 4), the CMC hydrogel presented a less rough surface. By grafting CMC with SSS,

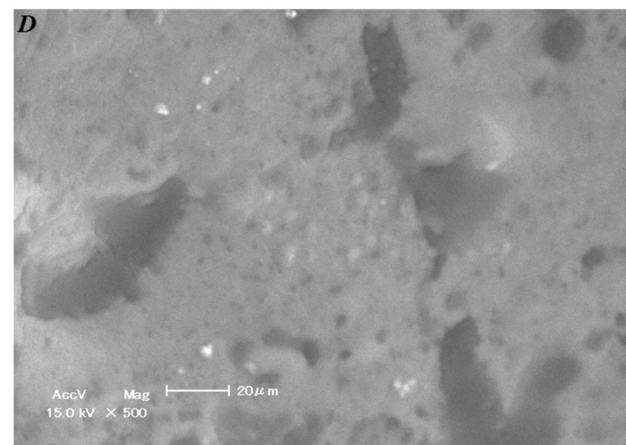
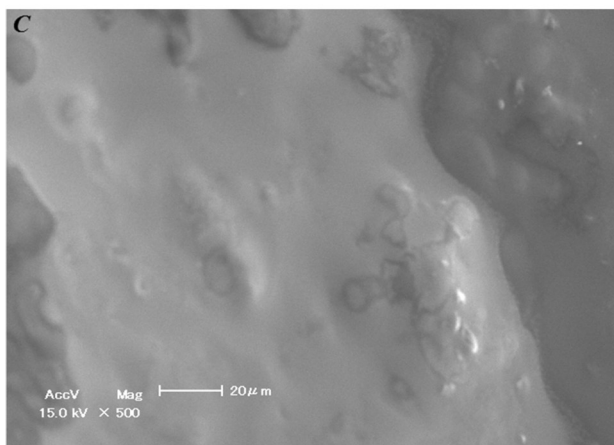
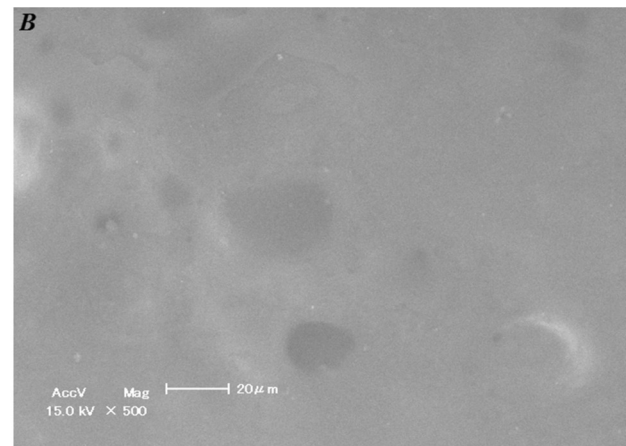
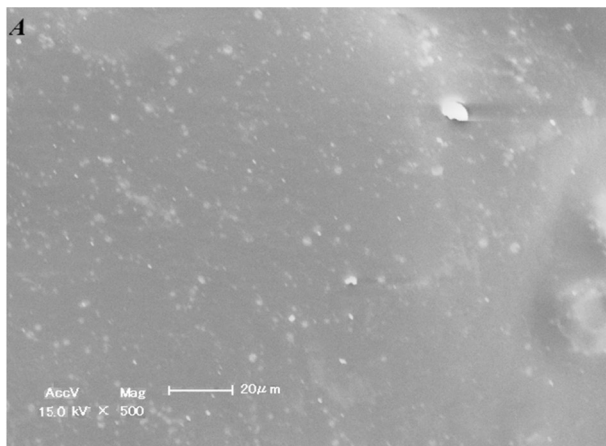


Fig. 4. SEM micrographs of CMC (A), CMC/SSS 2:1 (B), CMC/SSS 1:1 (C) and CMC/SSS 1:2 (D) hydrogels.

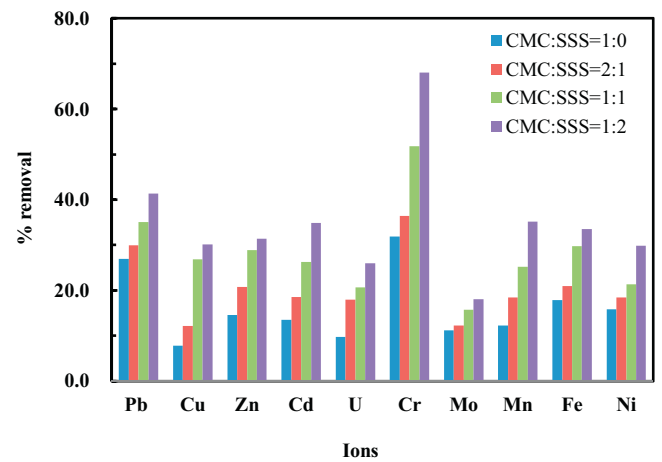


Fig. 5. Effect of hydrogel composition on the removal percentage of various metals.

the surface become rougher, more pores and hills with enhanced SSS and reduced CMC contents. Thus, comparison of these figures reveals that grafting has taken place.

### 3.3. Metal ion retention properties

#### 3.3.1. Effect of hydrogel composition

The nature of the adsorption depends on several factors: the adsorbents, initial feed concentration of metal ions or contact time, etc. Fig. 5 shows a clear dependence of metal ion uptake on copoly-

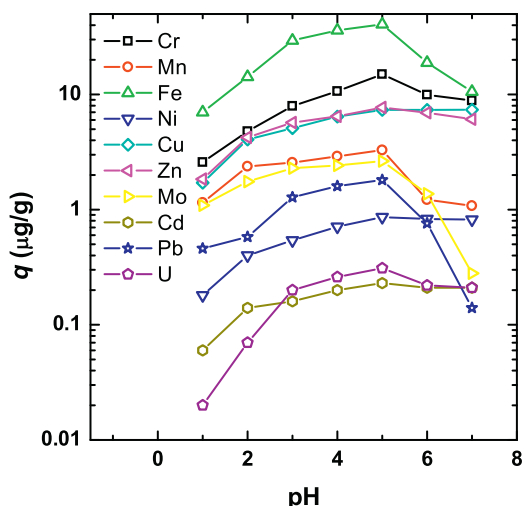


Fig. 6. Effect of pH on the adsorption of multi-elements onto CMC/SSS hydrogel.

mer hydrogel composition. As can be seen, the retention of metal ion increases with increasing SSS content. The CMC/SSS gels with ratio 1:2 showed high metal removal capacities at equilibrium for Cr (68.0%), Pb (41.4%), Mn (35.2%) and Fe (33.5%) compare with CMC gels, 31.9, 27.0, 12.3 and 17.9%, respectively. The CMC/SSS adsorbents did not present selectivity behavior for any specific metal ion except Cr (III), which means that the percentage removal does not depend on the metal ion's size even though the metal ions have different ionic radii, Pb (II) 133 pm and Mn (II) 81 pm. This behavior can be mainly due to the electrostatic interaction between the hydrophilic negatively charged sulfonic and carboxylic acid groups and the positively charged counter metal ions in the aqueous solution. The higher the valance of counter ions, the larger is the electrostatic attraction. Therefore, adsorbents tend to prefer counter ions of higher valence such as Cr (III). The higher metal ion removal of CMC/SSS gels in comparison with the CMC gels can be explained due to the presence of two groups, the sulfonic and carboxylic acid groups on the synthesized gels available to interact with the metal ions and remove them while CMC gels contain only a carboxylic group. In addition, sulfonic groups with  $pK_a < 1$  have much acid strength than carboxyl groups with  $pK_a \sim 4-5$  (Wilkins, 2006).

Another reason for the better performance of the CMC/SSS gels compared to the CMC gels is that the CMC/SSS gels have higher swelling capacities than the CMC gels. Therefore, the active groups will be more accessible and easier for metal ions in solution to diffuse into grafted gels.

### 3.3.2. Effect of adsorbate solution pH

The pH of the metal ions solution can influence strongly adsorption properties of hydrogel. This is because ion  $H_3O^+$  competing with the positively charged metal ions on the active sites of the adsorbent. From the results shown in Fig. 6, the adsorption capacities for the multi-elements onto CMC/SSS hydrogel increase sharply as the pH value of solution increases from 2 to 5 because the functional groups were deprotonated and are free to exchange or complex the metal ion (Rafatullah, Sulaiman, Hashim, & Ahmad, 2009). At the  $pH > 5$ , a decrease of adsorption for metal ions was observed due to metal precipitation appeared and the adsorbent was deteriorated with the accumulation of metal ions. Therefore, pH 5 was selected to be the optimum pH for further studies.

### 3.3.3. Kinetics

The kinetics of metal ions removal CMC/SSS gels indicated rapid binding of metal ions to the adsorbents during 10 h (Fig. 7), followed by a slow increase until equilibrium state was reached after 26 h and unchanged in equilibrium time up to 48 h. The initial rapid phase may be due to the increased number of vacant sites available at the initial stage. Generally, when adsorption involves a surface reaction process, the initial adsorption is rapid. Then, a slower adsorption would follow as the available adsorption site gradually decreases because of the pore diffusion of metal ions into the polymer matrix, i.e., intra-particle diffusion or chemical reaction would be the rate limiting step of sorption kinetics.

To elucidate the kinetics of the adsorption capacity of metal ions on grafted adsorbents at fixed concentration, the pseudo-first order kinetic model represented by the Lagergren Eq. (4) (Periasamy, 1994) and pseudo-second order kinetic model represented by the Eq. (5) (Ho & McKay, 1999) were used.

$$\frac{dq_t}{dt} = k_1 (q_e - q_t) \quad (4)$$

$$\frac{dq_t}{dt} = k_2 (q_e - q_t)^2 \quad (5)$$

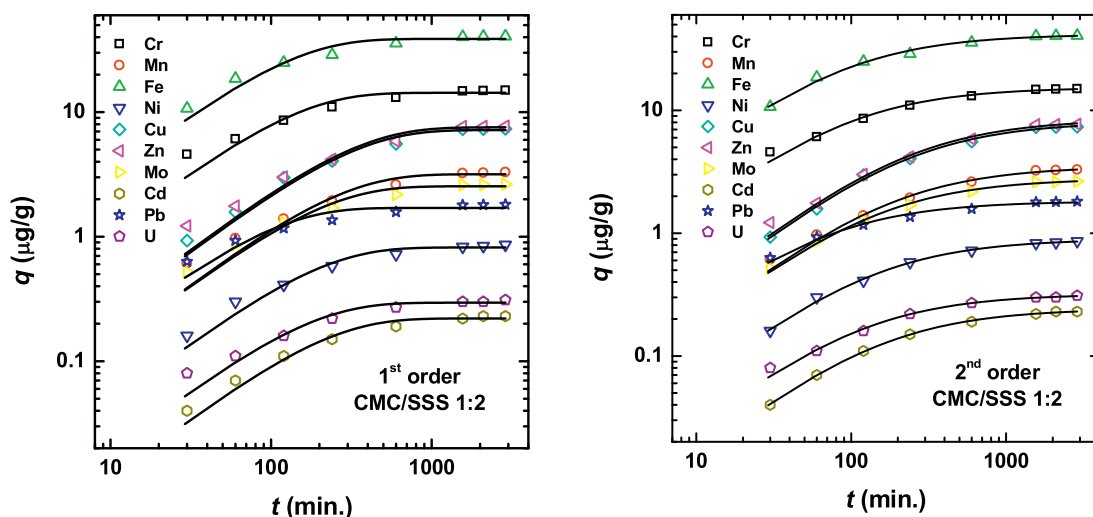


Fig. 7. Kinetics for the multi-element adsorption onto CMC/SSS gels.

**Table 2**  
Kinetic parameters of metal adsorption onto CMC/SSS adsorbent.

Metal	Pseudo-first-order model			$q_{ex}$ ( $\mu\text{g g}^{-1}$ )	Pseudo-second-order model		
	$q_{cal}$ ( $\mu\text{g g}^{-1}$ )	$k_1$ ( $\text{min}^{-1}$ )	$R^2$		$q_{cal}$ ( $\mu\text{g g}^{-1}$ )	$k_2$ ( $\text{g } \mu\text{g}^{-1} \text{min}^{-1}$ )	$R^2$
Cr	14.30	0.0080	0.968	14.97	15.38	0.0007	0.996
Mn	3.17	0.0044	0.976	3.29	3.51	0.0016	0.996
Fe	38.75	0.0086	0.964	40.65	41.67	0.0003	0.995
Ni	0.81	0.0058	0.981	0.86	0.90	0.0084	0.998
Cu	7.18	0.0035	0.983	7.34	8.01	0.0005	0.996
Zn	7.55	0.0035	0.981	7.71	8.48	0.0005	0.986
Mo	2.54	0.0054	0.976	2.64	2.78	0.0026	0.988
Cd	0.22	0.0053	0.983	0.23	0.24	0.0278	0.9989
Pb	1.70	0.0110	0.951	1.81	1.82	0.0087	0.993
U	0.29	0.0067	0.980	0.31	0.32	0.0285	0.997

where  $k_1$ ,  $k_2$  are the rate constants of adsorption,  $q_t$  and  $q_e$  are the amounts of metal adsorbed ( $\mu\text{g/g}$ ) at a time  $t$  and at equilibrium time (min.), respectively.

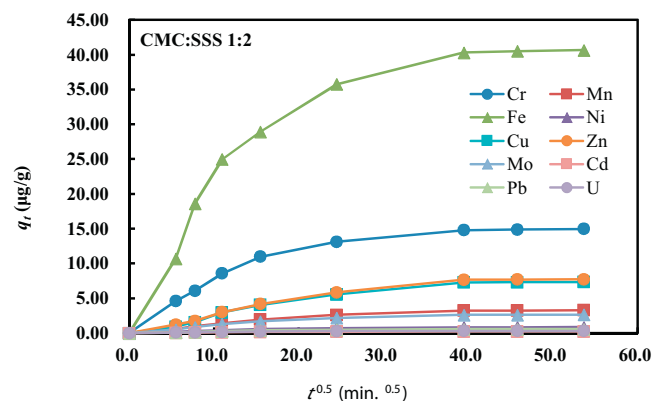
The kinetic parameters the pseudo-first-order and the pseudo-second-order models are shown in Fig. 7 and Table 2. Based on regression coefficient values ( $R^2$ ) and comparable theoretical and experimental  $q$  values, it can be said the pseudo-second-order kinetic model gave better fitting than the pseudo-first-order kinetic model. The results suggested that the pseudo-second-order adsorption mechanism dominated the adsorption process, and adsorption rates of metal ions onto gels were probably controlled by the chemical process, i.e. the chemisorptions involving valence forces through sharing or exchange of electrons between adsorbent and sorbate, not the physisorptions were significant (Ho & McKay, 1999). In fact, SSS has sulfonate group, therefore, the metal ion could be absorbed by interaction between the metal ion molecules and  $-\text{SO}_3^-$  groups of SSS. Furthermore, the calculated  $q_{cal}$  values for the pseudo-second-order kinetic model show good agreement with the experimental  $q_{ex}$  values.

The kinetic data were also applied to the Webber Morris intra-particle diffusion model (6) which is expressed as (Weber & Morris, 1963)

$$q_t = k_{id} \cdot t^{0.5} + C \quad (6)$$

where,  $q_t$  ( $\mu\text{g/g}$ ) is the amount of metal ions adsorbed at time  $t$ ,  $C$  is the intercept, and  $k_{id}$  is the intra-particle diffusion rate constant. The intra-particle diffusion model was proposed to identify the adsorption mechanism and to predict the rate-controlling step. If intra-particle diffusion is the sole rate-controlling step, the plot of  $q_t$  versus  $t^{0.5}$  will pass through the origin.

Fig. 8 shows the plot of the data obtained for the adsorption of multi-elements onto grafted hydrogels. The plot is not linear over the whole time range; however, it exhibits a tri-linearity, revealing the existence of three successive adsorption stages: (1) the initial steep phase represented surface diffusion; (2) the second less steep phase represented a gradual sorption of gels where

**Fig. 8.** Intra-particle diffusion model plots for multi-element sorption on to grafted gels.

intra-particle diffusion highly involved in the rate control of this mechanism; and (3) the final equilibrium phase where the intra-particle diffusion starts to slow down. This also has been observed by previous investigate (Chiou, Ho, & Li, 2004; Mishra, 2016; Olu-owolabi, Diagboya, & Adebawale, 2014). Since the second linear plots do not pass through the origin, intra-particle diffusion was not the only rate-limiting step. Some other processes may also control the rate of adsorption but only one predominates at any particular time phase. The values of the intra-particle diffusion rate constant, calculated from the slope of the straight line part of the curve.

### 3.3.4. Equilibrium isotherms

In order to evaluate the maximum metal ion uptake by grafted gel, adsorption isotherm experiments were conducted. The non-linear Langmuir and Freundlich models were employed most commonly (Benamer et al., 2011) to fit the resulted equilibrium data because they provide better fitting than the linear form (Ho, 2006).

**Table 3**  
Isotherm parameters for metal adsorption onto CMC/SSS gels.

Metal	Langmuir isotherm			Freundlich isotherm		
	$q_{max}$ ( $\mu\text{g/g}$ )	$k_L$ ( $\text{L}/\mu\text{g}$ )	$R^2$	$k_f$ ( $\mu\text{g/g}$ )	$n$	$R^2$
Cr	36.65	0.0140	0.970	2.2772	2.1176	0.899
Mn	8.78	0.0198	0.966	0.7027	2.2454	0.888
Fe	79.78	0.0054	0.990	6.1617	2.8610	0.913
Ni	2.67	0.0694	0.975	0.3051	1.9139	0.916
Cu	25.19	0.0061	0.986	0.7070	1.8222	0.940
Zn	30.34	0.0052	0.981	0.6592	1.7177	0.937
Mo	7.19	0.0107	0.976	0.3823	2.0980	0.918
Cd	0.42	0.5774	0.989	0.1682	2.9750	0.896
Pb	3.60	0.1514	0.984	0.8420	2.6940	0.890
U	0.58	0.7231	0.995	0.2515	2.7898	0.930

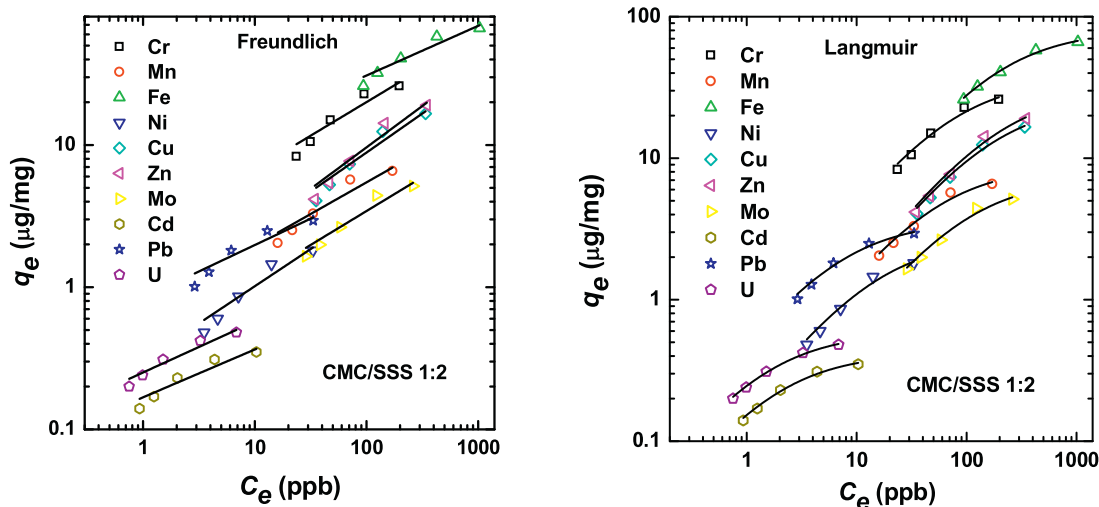


Fig. 9. Adsorption isotherm of metal ions by CMC/SSS gel.

The Langmuir isotherm is used to evaluate the sorption capacity of the chelating material. The linear form of this isotherm can be written as (7):

$$q_e = \frac{q_{max} \cdot k_L \cdot C_e}{1 + k_L \cdot C_e} \quad (7)$$

where  $C_e$  is the equilibrium concentration of adsorbate ( $\mu\text{g/L}$ ) and  $q_e$  is the amount adsorbed per gram of adsorbent at equilibrium ( $\mu\text{g/g}$ ),  $k_L$  is Langmuir isotherm constant ( $\text{L}/\mu\text{g}$ ) and  $q_{max}$  is the maximum monolayer coverage of metal ion capacity ( $\mu\text{g/g}$ ).

The Langmuir constant  $k_L$  of CMC/SSS gels is the adsorption equilibrium constant related to the affinity of the binding sites and energy of adsorption, which calculated to be highest for U (0.7231  $\text{L}/\mu\text{g}$ ). The stronger binding energy of U than others was ascribed to the stronger electrostatic interactions between U and adsorbent. As shown in Table 3, the maximum monolayer capacity of the CMC/SSS adsorbent for high removal of  $\text{Fe}^{2+}$ ,  $\text{Zn}^{2+}$  and  $\text{Cr}^{3+}$  were found to be 79.78, 30.34 and 36.65  $\mu\text{g g}^{-1}$ , respectively. The main reason for this priority could result from higher initial concentration. Similar trends are reported by other researcher (Ali, 2012).

The Freundlich equation used to evaluate heterogeneous surface energies is expressed as follows (8):

$$q_e = k_f \cdot C_e^{\frac{1}{n}} \quad (8)$$

where  $k_f$  indicates Freundlich constants is related to the adsorption equilibrium constant ( $\mu\text{g/g}$ ),  $C_e$  is the equilibrium concentration ( $\mu\text{g/L}$ ) and  $n$  an empirical parameter related to the intensity of adsorption, which varies with the heterogeneity of the adsorbent. The value  $k_f$  and  $n$  are also summarized in Table 3. The number of active sites  $n$  in the hydrogels for all investigated metal ions was greater than unit indicates that the sorption by hydrogels is favorable (Ramesh, Hasegawa, Sugimoto, Maki, & Ueda, 2008).

The metal ion uptake increased with increasing equilibrium concentrations (Fig. 9). By comparing the correlation coefficients in Table 3, it was found that the Langmuir isotherm model has a better fit compare to Freundlich model for CMC/SSS gels and this phenomenon suggests that the maximum monolayer adsorption takes place on the surface of the gels, rather than a multilayer adsorption.

#### 4. Conclusion

Heavy metal contamination has been a serious problem throughout the world because of the hazardous effects on the

health of humans. Even though there are well established techniques for the heavy metal removal from drinking water, their usage can be limited by cost. Hence, there exists a need to develop a method for heavy metal removal from aqueous solution which is cost effective, efficient and eco-friendly. We propose a novel method of using CMC grafted with SSS to remove heavy metals from water. Based on the results the following can be concluded:

- The CMC/SSS hydrogel was synthesized by using gamma irradiation. Water absorbency for this hydrogel showed higher than CMC hydrogel resulting from the  $-\text{COOH}$  and  $-\text{SO}_3\text{H}$  groups on the polymer chains.
- The hydrogel's functional groups revealed by spectroscopic analyses and later tested for adsorption properties included the carboxylate and sulfonate moieties. These groups enabled successful adsorption of metal ions from aqueous solution. The optimum pH value for metal uptake was around 6.
- The kinetics of adsorption process indicated that adsorption process was chemisorption process and monolayer sorption took place on the surface of the CMC/SSS hydrogel.

#### Acknowledgements

This work was supported by JSPS KAKENHI Grant Numbers 21656239, 24360398. The NMR measurement was performed by Evaluation Center of Materials Properties and Function, Kyushu University. The SEM observation was made using the SEM at the Center of Advanced Instrumental Analysis, Kyushu University.

#### References

- Abd El-Mohdy, H. L. (2007). Water sorption behavior of CMC/PAM hydrogels prepared by  $\gamma$ -irradiation and release of potassium nitrate as agrochemical. *Reactive and Functional Polymers*, 67(10), 1094–1102. <http://dx.doi.org/10.1016/j.reactfunctpolym.2007.07.002>
- Ali, A. E.-H. (2012). Removal of heavy metals from model wastewater by using carboxymethyl cellulose/2-acrylamido-2-methyl propane sulfonic acid hydrogels. *Journal of Applied Polymer Science*, 123, 763–769. <http://dx.doi.org/10.1002/app>
- Bao, Y., Ma, J., & Li, N. (2011). Synthesis and swelling behaviors of sodium carboxymethyl cellulose-g-poly(AA-co-AM-co-AMPS)/MMT superabsorbent hydrogel. *Carbohydrate Polymers*, 84(1), 76–82. <http://dx.doi.org/10.1016/j.carbpol.2010.10.061>
- Barakat, M. A. (2011). New trends in removing heavy metals from industrial wastewater. *Arabian Journal of Chemistry*, 4(4), 361–377. <http://dx.doi.org/10.1016/j.arabjc.2010.07.019>
- Benamer, S., Mahlous, M., Tahtat, D., Nacer-khodja, A., Arabi, M., Lounici, H., et al. (2011). Radiation synthesis of chitosan beads grafted with acrylic acid for



- metal ions sorption. *Radiation Physics and Chemistry*, 80(12), 1391–1397. <http://dx.doi.org/10.1016/j.radphyschem.2011.06.013>
- Chiou, M. S., Ho, P. Y., & Li, H. Y. (2004). Adsorption of anionic dyes in acid solutions using chemically cross-linked chitosan beads. *Dyes and Pigments*, 60(1), 69–84. [http://dx.doi.org/10.1016/S0143-7208\(03\)00140-2](http://dx.doi.org/10.1016/S0143-7208(03)00140-2)
- Crini, G. (2005). Recent developments in polysaccharide-based materials used as adsorbents in wastewater treatment. *Progress in Polymer Science (Oxford)*, 30(1), 38–70. <http://dx.doi.org/10.1016/j.progpolymsci.2004.11.002>
- Ghosh, P., Dev, D., & Samanta, A. K. (1995). Graft copolymerization of acrylamide on cotton cellulose in a limited aqueous system following pretreatment technique. *Journal of Applied Polymer Science*, 58, 1727–1734.
- Gu, G. (2001). Graft copolymerization of acrylic acid onto cellulose: Effects of pretreatments and crosslinking agent. *Journal of Applied Polymer Science*, (March) <http://dx.doi.org/10.1002/app.1331>
- Gupta, K. C., & Sahoo, S. (2001). Graft copolymerization of acrylonitrile and ethyl methacrylate comonomers on cellulose using ceric ions. *Biomacromolecules*, 2, 239–247.
- Ho, Y. S., & McKay, G. (1999). Pseudo-second order model for sorption processes. *Process Biochemistry*, 34(5), 451–465. [http://dx.doi.org/10.1016/S0032-9592\(98\)00112-5](http://dx.doi.org/10.1016/S0032-9592(98)00112-5)
- Ho, Y. S. (2006). Isotherms for the sorption of lead onto peat: Comparison of linear and non-linear methods. *Polish Journal of Environmental Studies*, 15(1), 81–86. <http://dx.doi.org/10.1016/j.watres.2005.10.040>
- Korus, I. (2012). Heavy metals complexes of poly (sodium 4-styrenesulfonate)—thermogravimetric studies. *Polymer*, 57, 290–295.
- Kumar, R., Setia, A., & Mahadevan, N. (2012). Grafting modification of the polysaccharide by the use of microwave irradiation—A review. *International Journal of Recent Advances in Pharmaceutical Research*, 2(April), 45–53.
- Liu, P., Borrell, P. F., Božič, M., Kokol, V., Oksman, K., & Mathew, A. P. (2015). Nanocelluloses and their phosphorylated derivatives for selective adsorption of Ag<sup>+</sup>, Cu<sup>2+</sup> and Fe<sup>3+</sup> from industrial effluents. *Journal of Hazardous Materials*, 294, 177–185. <http://dx.doi.org/10.1016/j.jhazmat.2015.04.001>
- Ma, H., Hsiao, B. S., & Chu, B. (2012). Ultrafine cellulose nanofibers as efficient adsorbents for removal of UO<sub>2</sub><sup>2+</sup> in water. *ACS Macro Letters*, 1, 213–216. <http://dx.doi.org/10.1021/mz200047q>
- Mishra, S., Rani, G. U., & Sen, G. (2012). Microwave initiated synthesis and application of polyacrylic acid grafted carboxymethyl cellulose. *Carbohydrate Polymers*, 87(3), 2255–2262. <http://dx.doi.org/10.1016/j.carbpol.2011.10.057>
- Mishra, A. K. (2016). *Smart materials for waste water applications*. Wiley. Retrieved from. <https://books.google.com/books?id=Af2OCwAAQBAJ&pgis=1>
- Mondal, I. H. (2013). Grafting of methyl acrylate and methyl methacrylate onto jute fiber: Physico-chemical characteristics of the grafted jute. *Journal of Engineered Fibers and Fabrics*, 8(3), 42–50.
- Morales, D. V., & Rivas, B. L. (2014). Poly (Acrylamide-co-styrene sodiumsulfonate) and poly (2-acrylamide-2-methyl-1-propanesulfonic acid-co-acrylic acid) resins with removal properties for Hg(II), Pb(II), Cd(II), and Zn(II). *Journal of Chilean Chemical Society*, 59(2), 2420–2426.
- Ogbeifun, D. E., & Okieimen, F. E. (2004). *Synthesis, characterisation and flocculation properties of carboxymethyl cellulose-g acrylamide*. *Iran Journal of Science*, 15(1), 53–57.
- Olu-owolabi, B. I., Diagboya, P. N., & Adebowale, K. O. (2014). Evaluation of pyrene sorption e desorption on tropical soils. *Journal of Environmental Management*, 137, 1–9. <http://dx.doi.org/10.1016/j.jenvman.2014.01.048>
- Periasamy, K. (1994). Process development for removal and recovery of cadmium from wastewater by a low-cost adsorbent: Adsorption rates and equilibrium studies. *Industrial & Engineering Chemistry Research*, 33, 317–320.
- Pushpamalar, V., Langford, S. J., Ahmad, M., & Lim, Y. Y. (2006). Optimization of reaction conditions for preparing carboxymethyl cellulose from sago waste. *Carbohydrate Polymers*, 64(2), 312–318. <http://dx.doi.org/10.1016/j.carbpol.2005.12.003>
- Rafatullah, M., Sulaiman, O., Hashim, R., & Ahmad, A. (2009). Adsorption of copper (II), chromium (III), nickel (II) and lead (II) ions from aqueous solutions by meranti sawdust. *Journal of Hazardous Materials*, 170(2–3), 969–977. <http://dx.doi.org/10.1016/j.jhazmat.2009.05.066>
- Ramesh, A., Hasegawa, H., Sugimoto, W., Maki, T., & Ueda, K. (2008). Adsorption of gold(III), platinum(IV) and palladium(II) onto glycine modified crosslinked chitosan resin. *Bioresource Technology*, 99(9), 3801–3809. <http://dx.doi.org/10.1016/j.biortech.2007.07.008>
- Rivas, B. L., & Muñoz, C. (2009). Synthesis and metal ion adsorption properties of poly(4-sodium styrene sulfonate-co-acrylic acid). *Journal of Applied Polymer Science*, 114(3), 1587–1592. <http://dx.doi.org/10.1002/app.30722>
- Sehaqui, H., de Larraya, U. P., Liu, P., Pfenninger, N., Mathew, A. P., Zimmermann, T., et al. (2014). Enhancing adsorption of heavy metal ions onto biobased nanofibers from waste pulp residues for application in wastewater treatment. *Cellulose*, 21(4), 2831–2844. <http://dx.doi.org/10.1007/s10570-014-0310-7>
- Sultana, S., Islam, M. R., Dafader, N. C., & Haque, M. E. (2012). Preparation of carboxymethyl cellulose/acrylamide copolymer hydrogel using gamma radiation and investigation of its swelling behavior. *Journal of Bangladesh Chemical Society*, 25(2), 132–138.
- Wang, W., & Wang, A. (2011). Preparation, swelling, and stimuli-responsive characteristics of superabsorbent nanocomposites based on carboxymethyl cellulose and rectorite. *Polymers for Advanced Technologies*, 22(12), 1602–1611. <http://dx.doi.org/10.1002/pat.1647>
- Weber, W. J., & Morris, J. C. (1963). Kinetics of sorption of carbon from solution. *Kinetics of Sorption*, 89, A2–SA31.
- Wilkins, L. W. (2006). *Remington: The science and practice of pharmacy*. Lippincott Williams & Wilkins. Retrieved from. <https://books.google.com/books?id=NFGSSBaWjwC&pgis=1>
- Yoshii, F., Zhao, L., Wach, R. A., Nagasawa, N., Mitomo, H., & Kume, T. (2003). Hydrogels of polysaccharide derivatives crosslinked with irradiation at paste-like condition. *Nuclear Instruments and Methods in Physics Research Section B: Beam Interactions with Materials and Atoms*, 208, 320–324. [http://dx.doi.org/10.1016/S0168-583X\(03\)00624-4](http://dx.doi.org/10.1016/S0168-583X(03)00624-4)